JOURNAL OF AGRICULTURAL AND FOOD CHEMISTRY

Article

pubs.acs.org/JAFC

Understanding the Molecular Signatures in Leaves and Flowers by Desorption Electrospray Ionization Mass Spectrometry (DESI MS) Imaging

R. G. Hemalatha and T. Pradeep*

DST Unit on Nanoscience and Thematic Unit of Excellence, Department of Chemistry, Indian Institute of Technology Madras, Chennai, India

Supporting Information

ABSTRACT: The difference in size, shape, and chemical cues of leaves and flowers display the underlying genetic makeup and their interactions with the environment. The need to understand the molecular signatures of these fragile plant surfaces is illustrated with a model plant, Madagascar periwinkle (*Catharanthus roseus* (L.) G. Don). Flat, thin layer chromatographic imprints of leaves/petals were imaged using desorption electrospray ionization mass spectrometry (DESI MS), and the results were compared with electrospray ionization mass spectrometry (ESI MS) of their extracts. Tandem mass spectrometry with DESI and ESI, in conjunction with database records, confirmed the molecular species. This protocol has been extended to other plants. Implications of this study in identifying varietal differences, toxic metabolite production, changes in metabolites during growth, pest/pathogen attack, and natural stresses are shown with illustrations. The possibility to image subtle features like eye color of petals, leaf vacuole, leaf margin, and veins is demonstrated.

KEYWORDS: *molecular imaging, surface-bound metabolites, electrospray ionization (ESI), desorption electrospray ionization (DESI), mass spectrometry (MS)*

INTRODUCTION

Underlying the incredible beauty of leaves and flowers is their enormous chemical complexity. Various mysteries in plant chemical biology are solved by breakthrough techniques. Different methods of mass spectrometry have contributed significantly to the detection, identification, and quantification of important biomolecules, biomarkers, and other metabolites; even their spatial distribution on surfaces may be visualized with the latest techniques of mass spectrometry imaging (MSI). There are variations in principle, application, and versatility in all the three different mass spectrometric techniques used in MSI, namely secondary ion mass spectrometry (SIMS), matrix-assisted laser desorption ionization mass spectrometry (MALDI MS), and desorption electrospray ionization mass spectrometry (DESI MS).[1] The application of MALDI MSI is high in pharmaceutical research but its major application in plants is for imaging proteins. SIMS imaging in plants has revealed the possibility to get detailed elemental mapping of water and nutrients (major, minor nutrients and other trace elements) in addition to the imaging of molecules like epicuticular waxes, lipids, flavones, and other selected categories of metabolites. DESI MS is distinctly different and often advantageous in biological applications as the process of ionization occurs in ambient conditions and the samples need not be prepared for analysis.[2] More recent studies have demonstrated the need for variations of surfaces, solvents, and methods to suit various plant parts like roots, stems, fruits, bulbs, and rhizomes.[3−9] However, researchers have measured only a limited number of bioactive molecules so far, which have been possible by the chosen techniques, tools, and the technical capacity of particular instrument models available at that time.

Numerous experiments have been performed to understand the response and mechanism of crop plants' survival in various biotic and abiotic stress conditions. It is obvious that the plant surfaces display some changes in color, shape, and stunted growth, etc., when the plants undergo multifaceted stressful conditions. Hence there is specific need to measure the molecular signatures of fragile plant surfaces under healthy conditions and compare their transient changes in conditions of stress. Here we suggest DESI MS based thin layer chromatography (TLC) imprint-imaging as a rapid method for studying metabolites on plant surfaces. The strategy is illustrated with the model plant, Madagascar periwinkle - *Catharanthus roseus* (L.) G. Don. It bears flowers throughout the year, and the whole plant is a rich source of natural alkaloids. Decades of research on *Catharanthus* alkaloids continues even now, because of their high market value and proven potential in the treatment of different types of cancer. It is used as a model for rapid identification of commercially exploited alkaloids that could be engineered to form "differently" from the same indole alkaloid metabolic pathway.[10] Following the recently developed imprint imaging method of DESI MS,[11−13] here, the TLC-imprints of petals and leaves were used to get highly specific, spatially resolved analysis of molecular signatures of *C. roseus*. In addition to DESI MS imaging, tandem mass spectra (MS/MS) were collected from periwinkle leaf/petal extracts and compared with the reports in

Received: March 24, 2013
Revised: July 11, 2013
Accepted: July 12, 2013
Published: July 12, 2013

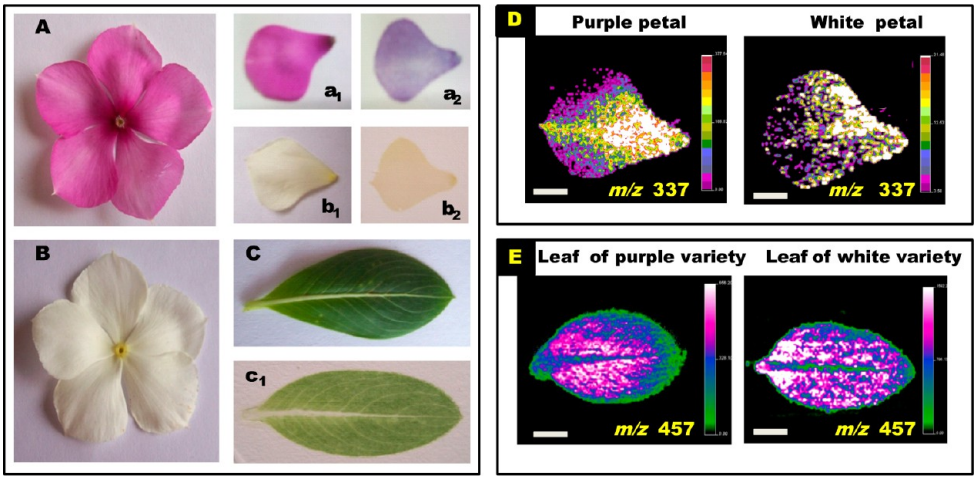

Figure 1. Photographs of flowers, petals, and a leaf of Madagascar periwinkle *C. roseus* and their TLC imprints: Images of (A) pink flower, (a_1) single petal of a pink flower, and (a_2) TLC-imprint of a pink petal. Images B, b_1, and b_2 correspond to the same data for a white flower. Images C and c_1 correspond to a leaf and its imprint. Imprints do not correspond to the same petals or leaf whose photographs are shown. Images D and E correspond to one of the DESI MS images collected from petal and leaf showing the difference in spatial distribution between purple and white varieties of periwinkle, using the ion at m/z 337 and 457, respectively. Scale bars of both the images in D and E are the same (5 mm).

databases. The changes in the spatial distribution of selected metabolites during pest/pathogen attack and under natural stress were imaged. Besides Madagascar periwinkle, different plants like tomato, potato, *Arabidopsis*, tamarind, coriander, amaranthus, neem, patchouli, and wedelia were imaged for their molecular signatures to demonstrate specific applications.

MATERIALS AND METHODS

Materials and Reagents. Leaves and flowers of *C. roseus* and leaves of tomato (*Lycopersicon esculentum* L.), potato (*Solanum tuberosum* L.), tamarind (*Tamarindus indicus* L.), coriander (*Coriandrum sativum* L.) amaranthus (*Amaranthus viridis* L.), neem (*Azadirachta indica* A. Juss.), and wedelia (*Wedelia trilobata* (syn. *Sphagneticola trilobata* L.)) were collected from plants that were growing in the nursery of IIT Madras campus situated in Chennai, Tamilnadu state, India. The plant patchouli (*Pogostemon cablin* (Blanco) Benth.) was a gift from Prof. Vasundhara Mariappa (University of Agricultural Sciences, Bangalore). Tissue cultured plants of *Arabidopsis thaliana* were received as gift from Dr. Baskar (Biotechnology Department, IIT Madras). Methanol and acetonitrile of HPLC grade were purchased from Standard Reagents Pvt. Ltd., Hyderabad, India, and RFCL Limited, New Delhi, India, respectively. TLC plates (Silica gel 60 F_{254} aluminum sheet, 20 × 20 cm) were purchased from Merck KGaA, Darmstadt, Germany. Deionized water was used for making solutions.

Preparation of TLC-Imprints. Fresh plant sample (leaf/petal) with its upper or lower surface facing the silica coating, as per requirement, was placed on the TLC plate of specific dimension. The TLC plate−plant sample pair was covered on either side with tissue paper and manually imprinted using a laboratory hydraulic pellet press by applying a load of 1 ton and 3 tons over an area of 2.5 cm^2 for petals and leaves, respectively, for a period of approximately 5−10 s. The load was optimized individually based on sample physical features (based on the time of collection, surface dryness, and thickness of the leaf/petal). Optimization was necessary as petals required lower load in comparison to leaves. A transparent layer was separated after the release of applied pressure. This layer is due to the waxy coating of the leaf/petal. It was important that the loads were uniform so that the imprints made a true representation of the chemical signatures of the sample (Figure 1 and Figure S1 (Supporting Information)).

Instrumental Setup. Each TLC imprint with the rectangular area occupied by the sample chemical imprint was mapped with optimized spatial resolution (one pixel: 400 μm^2 or 20 × 20 μm) in a lab-built 2D moving stage DESI source, as described earlier.[11−13] Different solvents and mixtures like methanol, methanol−water (3:1 v/v), and acetonitrile were used as spray solvents and delivered at a flow rate of 2 μL/min. Mass spectra were acquired in full scan, positive ion mode, over the mass range from m/z 50 to 1000, using a Thermo LTQ mass spectrometer (San Jose, CA). Auto gain control (AGC) was set to off, and each mass spectrum was collected with optimized scan time. The mass spectra collected as Xcalibur raw data were processed with FireFly data conversion software (http://www.prosolia.com/firefly.php), and images were viewed using BioMap (http://www.maldimsi.org). Tandem mass spectrometric studies were conducted using an ESI attachment of the same Thermo LTQ mass spectrometer, and the data were acquired with Xcalibur software. The plant (leaf and petal) extracts were prepared in ppm concentrations by immersing the leaf/petal in the solvents and solvent mixtures mentioned for an optimized time interval. The centrifuged plant extracts were electrosprayed at a flow rate of 10 μL/min with a spray voltage of 4.5 kV. Mass spectra were acquired for a full scan range of m/z 50−1000, and MS^2 scans were done on all the dominant peaks. To identify the metabolite, the experimental details of MS^2 scans of each peak was submitted to MS/MS spectrum search option of databases,[14−16] with user defined precursor mass and one or more cation/anion adducts. For example, in the METLIN database, the list of adducts given for positive ionization mode are as follows: M + Na, M + NH_4, M + H − $2H_2O$, M + H − H_2O, M + ACN + H, M + 2Na − H, M + 2H, M + 3H, M + H + Na, M + 2H + Na, M + 2Na, M + 2Na + H, M + Li, and M + CH_3OH. For negative ionization, the choices are as follows: M − H, M − H_2O − H, M + Na − 2H, M + Cl, M + K − 2H, M + FA − H, M − 2H, M − 3H, M + CH_3COO, and M + F (The acronyms correspond to ACN = aceonitrile, FA = formic acid). [15]

RESULTS AND DISCUSSION

Direct detection of molecules from plants is known from DESI MS imaging and other recent strategies.[3−9] Yet imaging fragile, short-lived plant surfaces like flower petals and thin leaves like coriander is difficult as they cannot be handled easily on a sample stage. Since ambient imaging with DESI MS requires flat surfaces for a true representation of the molecular concentrations, the plant surfaces were imprinted on TLC plates. Li et al.[12] and Thunig et al.[13] reported that imprints on porous Teflon gave good, stable, and intense signals when compared to direct imaging of plants. Here, besides enhancement in signal, TLC-imprints were ideal for imaging fragile

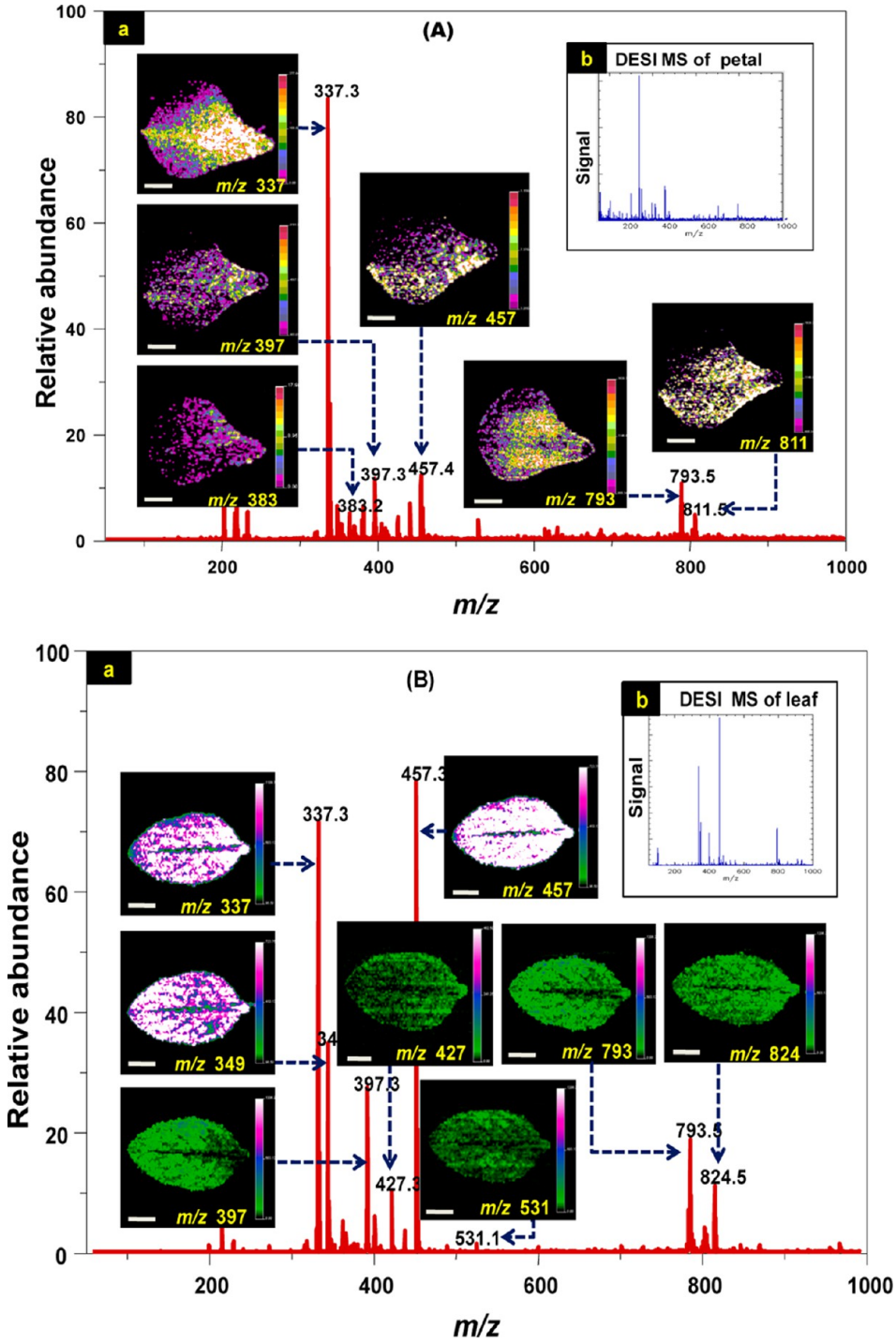

Figure 2. Distribution of metabolites on (A) petal and (B) leaf of *C. roseus*. (A) (a) ESI MS spectrum of petal of *C. roseus*. (b) One of the DESI MS spectra collected from a petal during imaging, corresponding to one pixel (400 μm^2) of the image. Images corresponding to various peaks are shown. Similar data for a leaf is shown in B. The scale is uniform in all the images (5 mm).

plant surfaces, and imprints themselves could be stored for further reference. TLC plates with silica gel coatings are preferable because they provided good quality imprints besides giving good adsorption of different plant-derived molecules and observable chemical changes with time. Figure 1 and Figure S1 of the Supporting Information show that TLC-imprints are truly reflecting the surface. Parts A and B of Figure 1 show the actinomorphic flower (having five identical petals) in pink and white colored varieties of periwinkle. The metabolites on the upper surface of single petal, leaf, and flower could be imprinted (Figure 1a_2, b_2, c_2; no. 2 in Figure S1A) to identify the difference in spatial distribution of specific metabolite between two colored varieties (Figure 1C,D). The undersurface of the petal is transparent (no. 1 in Figure S1A). Applying pressure on the undersurface of petal did not give good imprints (no. 3 in Figure S1A); but in leaves, both surfaces had metabolites (nos. 4, 5 in Figure S1A). Whether petal or leaf, a transparent layer (nos. 6, 7 of Figure S1A) could be separated after imprinting. Likewise, when the plant leaf/petal was kept dipped in solvents for long time, all molecular species got

dx.doi.org/10.1021/jf4011998 | J. Agric. Food Chem. 2013, 61, 7477−7487

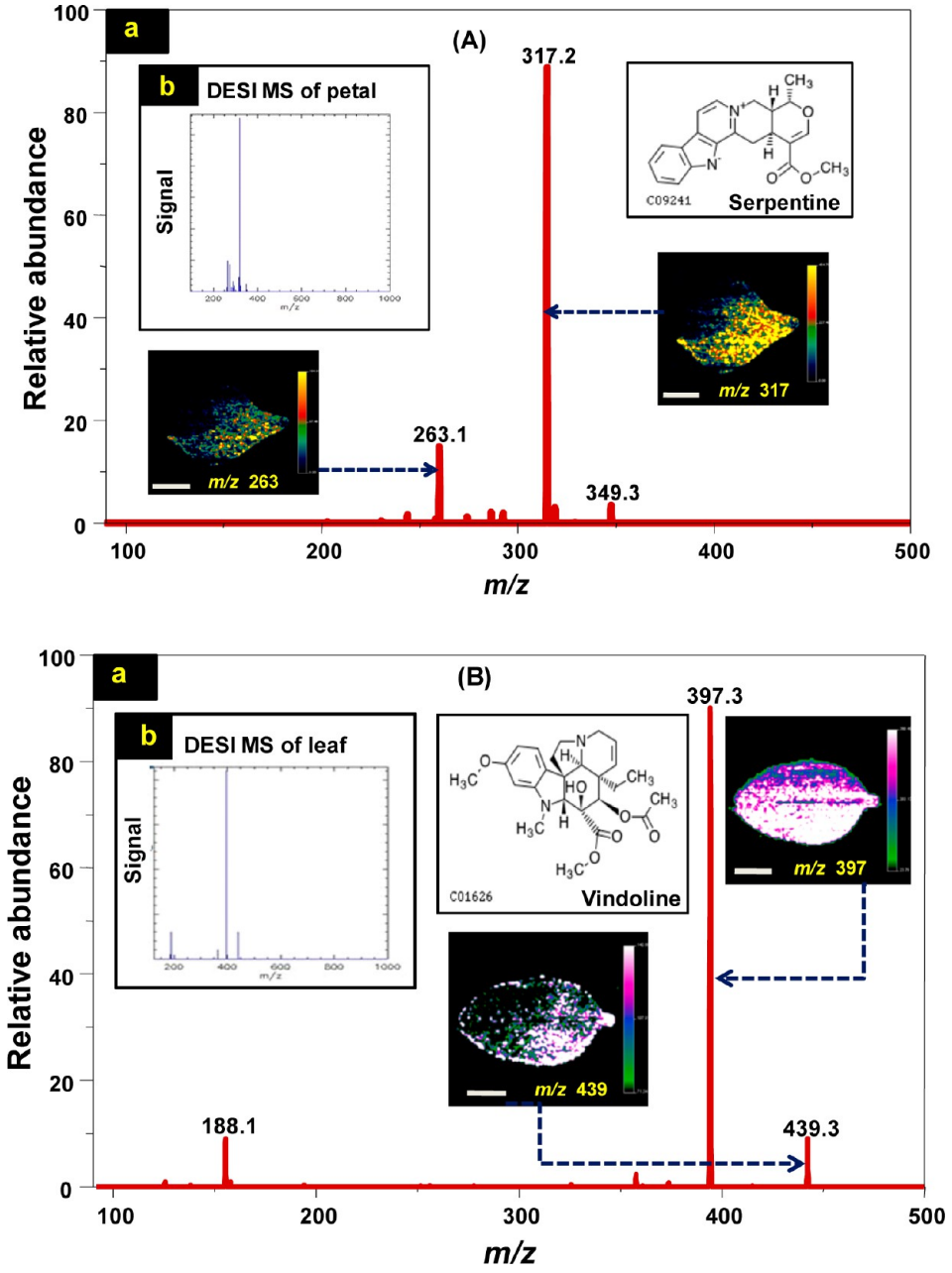

Figure 3. ESI MS tandem mass spectra and DESI MS tandem mass spectral images for (A) serpentine (m/z 349)) on the petal and (B) vindoline (m/z 457) on the leaf of *C. roseus*. The markings on the structures in insets of A and B are from the KEGG database.[21] The main figure corresponds to the spectrum, and the images are based on the intensities of the peaks marked. The spectrum from a pixel of the image is shown in the inset. The scale is uniform in all the images (5 mm).

extracted leaving behind the respective thin membranes. Imaging of TLC-imprints with intact thin membrane did not produce any images though some peaks were detected with low intensity. For easy identification of small molecular metabolites on plant surfaces, typical model plant species like potato, tomato, and *Arabidopsis* with already known bioactive compounds and pathways were chosen. However, the present study is primarily focused on the plant *C. roseus* because the availability of flowers throughout the year helped to do and/or repeat experiments anytime. The suitability of this method to tree species or even weed species is also checked with suitable examples (trees: tamarind, neem; weed: wedelia). Very small flowers like that of neem and *Arabidopsis* could not be imaged. The plant parts like stem, seed, etc. are not suitable for a direct imprinting method described here and need some modified processes which are not discussed here. In all of these selected plants, it is possible to get images for the already reported compounds from plants (indole alkaloids: Madagascar periwinkle; sesquiterpene lactones: wedelia; limonoid terpenes: neem; flavone glycosides: tamarind; polyphenols: coriander; betacyanins: amaranthus; aromatic oils: patchouli) when the same instrumental conditions and solvents were used as per the reports.[17−25] As the DESI MS data are voluminous, only images of the crucial metabolites (in all selected plants) for specific applications are presented (Figures 1−6 and Figures S1−S3 for *C. roseus* and in Figures 4C,D and Figures 6A−P for other plants).

dx.doi.org/10.1021/jf4011998 | *J. Agric. Food Chem.* 2013, 61, 7477−7487

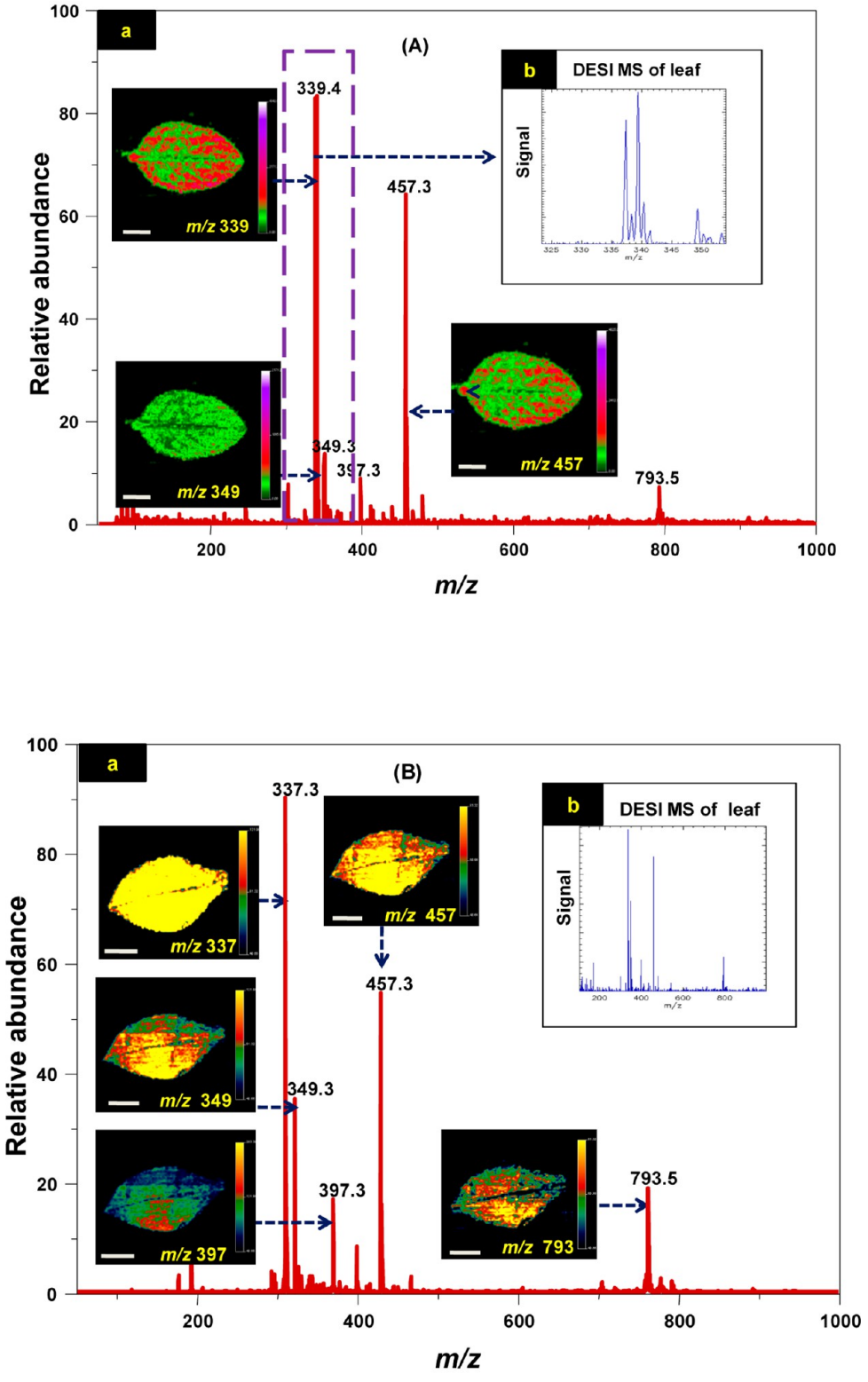

Figure 4. continued

dx.doi.org/10.1021/jf4011998 | J. Agric. Food Chem. 2013, 61, 7477−7487

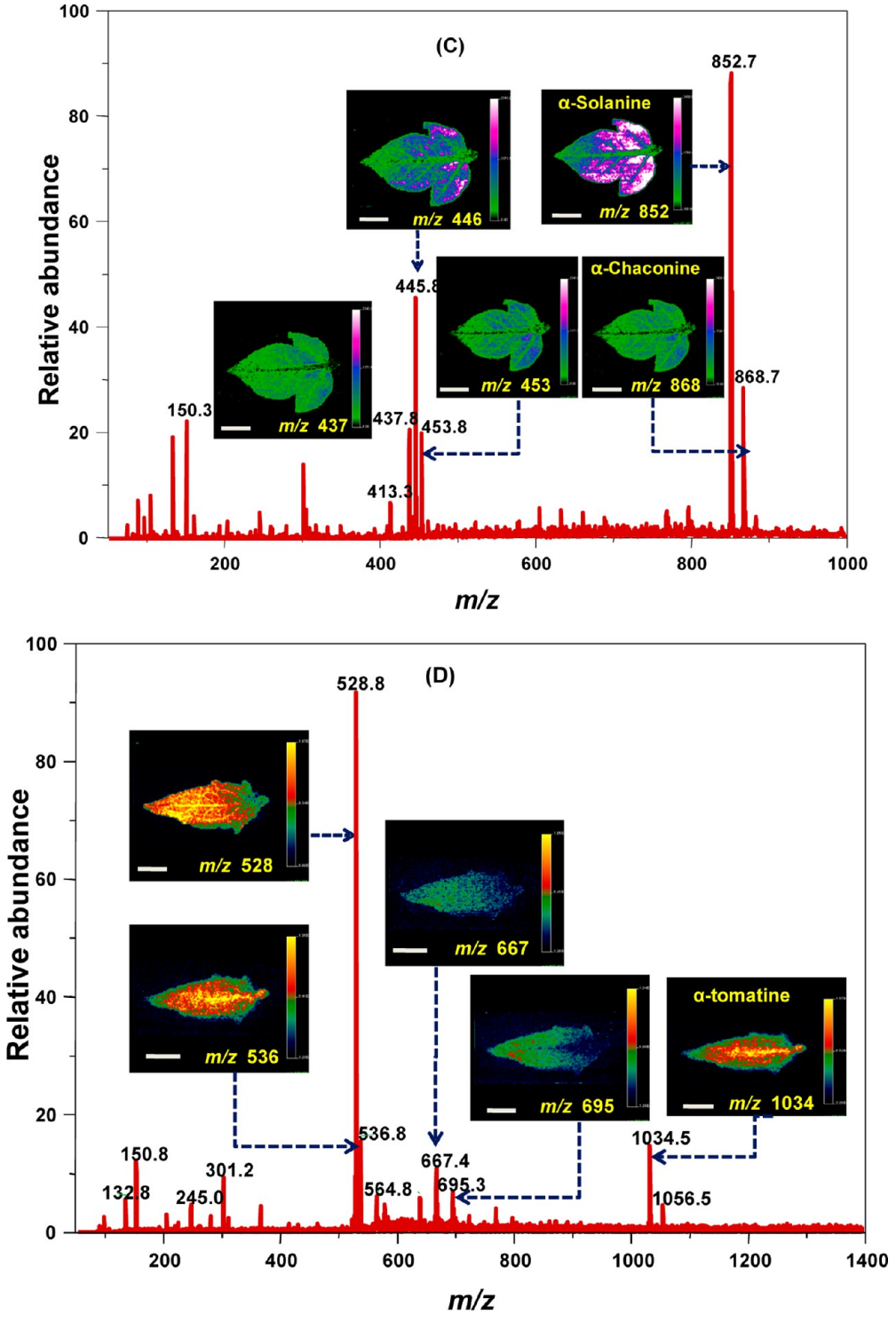

Figure 4. Distribution of selected metabolites on (A) newly emerged leaf and (B) senescent leaf of *C. roseus*. (A) (a) ESI MS spectrum of the leaf of *C. roseus*. Dotted portion is expanded in the inset. (b) One of the DESI MS spectra collected from a leaf during imaging, corresponding to one pixel (400 μm^2) of the image. Similar data for a senescent leaf is shown in B. Distribution of glycoalkaloid in (C) three-leaved stage seedling of potato and (D) mature leaf of tomato. Images corresponding to various peaks are shown. The scale is uniform in all the images (5 mm).

Parts A and B of Figure 2 show the spatial distribution of different metabolite peaks on the petal and leaf of *C. roseus*, detected in positive ionization mode using methanol as the spray solvent. The predominant presence of *m*/*z* 337 on petals (Figure 2A) and *m*/*z* 457 on the leaf (Figure 2B) is revealed. To identify all the eluted peaks, experiments with tandem mass spectral imaging were required. In *C. roseus*, alkaloids were chosen because of their high demand and widespread uses in clinical medicine. Here, the already available indole alkaloid pathway of KEGG (Kyoto Encyclopedia of Genes and Genomes)[21] was used, and the tandem mass spectra of the reported alkaloids were identified. Parts A and B of Figure 3 show the tandem mass spectral images for serpentine and vindoline, which matched with the characteristic ESI MS/MS

dx.doi.org/10.1021/jf4011998 | J. Agric. Food Chem. 2013, 61, 7477−7487

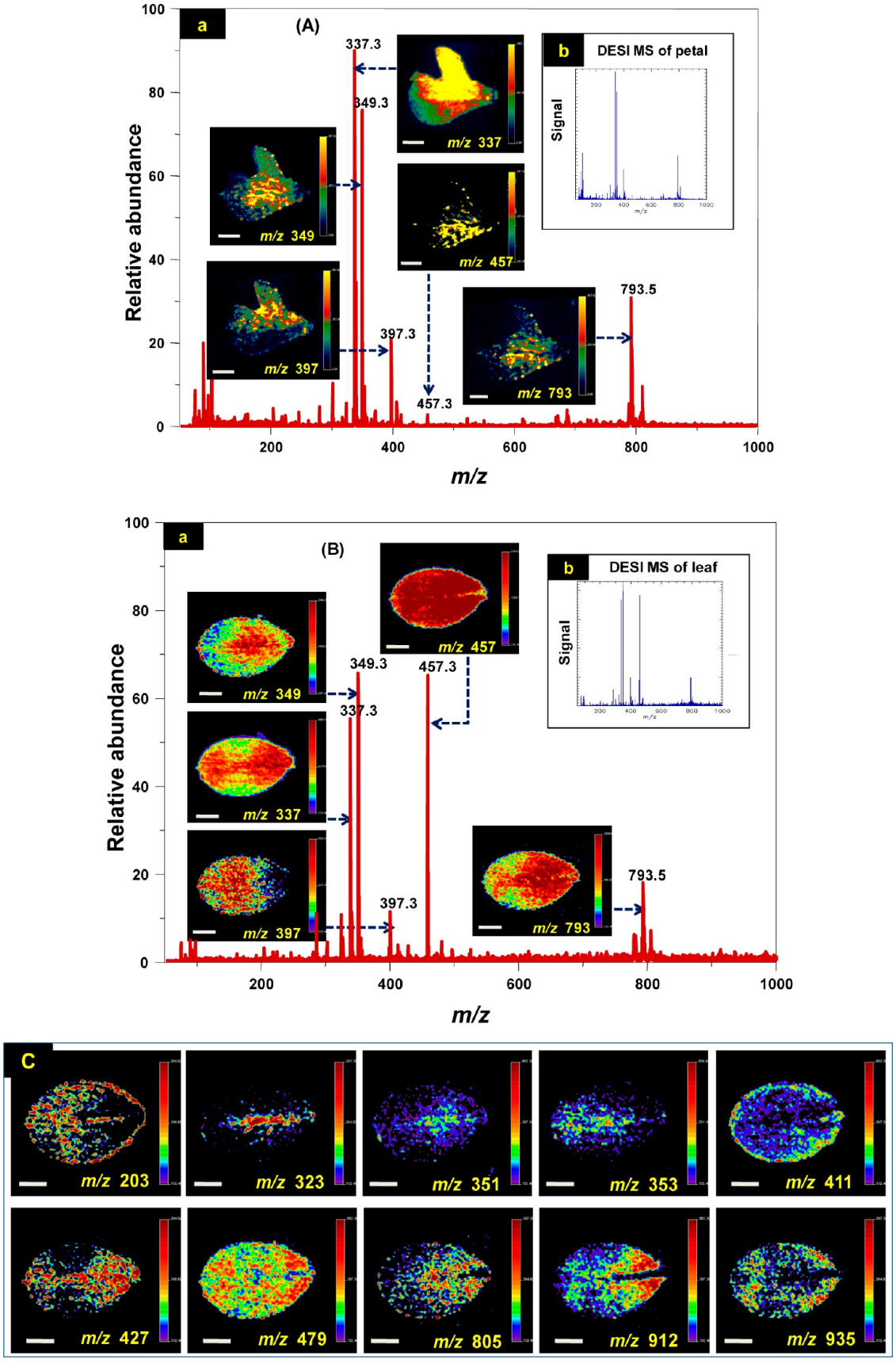

Figure 5. continued

dx.doi.org/10.1021/jf4011998 | J. Agric. Food Chem. 2013, 61, 7477−7487

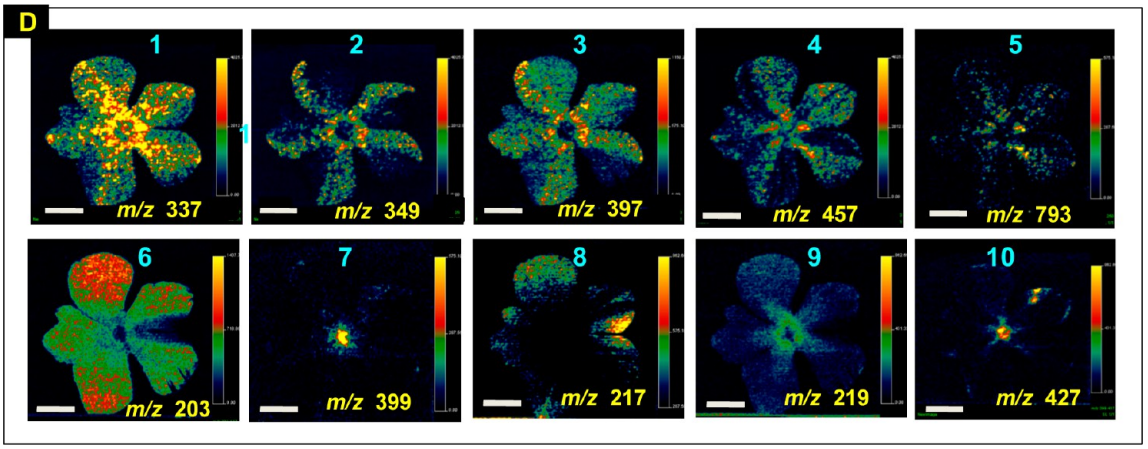

Figure 5. ESI MS spectrum and DESI MS images showing the distribution of selected metabolites during (A) grasshopper attack on petal and (B) wilt disease on leaf of *C. roseus*. (A) (a) ESI MS spectrum of petal. (b) One of the DESI MS spectra collected from the pest attacked petal during imaging corresponding to one pixel (400 μm^2) of the image. Similar data for a diseased leaf is shown in B. (C) DESI MS images of insignificant peaks (relative abundance <10%) in wilt disease. (D) DESI MS images showing distribution of selected metabolite peaks in atrophied flower (no. 1 of Figure S1C) of *C. roseus* during environmental stress. The scale is uniform in all the images (5 mm).

data of plant extracts and the diagnostic fragments available in databases.[18−22] The metabolite peak *m/z* 337 is sharing the tandem mass spectral peak positions of catharanthine and 19-S-vindoline with their characteristic MS/MS data (Figure S2a). As plants may contain complex mixtures under natural conditions, their tandem mass spectral data do not comply fully with the synthetic standards. The metabolites sharing the same *m/z* values (like catharanthine and tabersonine isomers for *m/z* 337, dihydrotabersonine and perivine for *m/z* 339, serpentine and alstonine for *m/z* 349, ajmalicine and hydroxy tabersonine for *m/z* 353, and decaetoxyvindoline and S-adenosyl methionine for *m/z* 399) which may be from the same indole alkaloid or other pathway(s) can also be delineated with their characteristic MS/MS data in databases. The ESI MS/MS of selected peaks are given in Figure S2. The results generated during MS/MS data searches in databases were voluminous when all possible adducts (examples given in the Materials and Methods section) were selected as user inputs; hence only protonated ions are given in this article. The fragmentation patterns of natural compounds are useful in drug discovery,[26] and studies show that modifications of the structure of vindoline lead to a range of antitumor alkaloids (like vinblastine, vincristine, vinorelbine, and vinflunine, etc.)[27] The other peaks that could be assigned using MS/MS spectrum search include akuammicine (*m/z* 323), serpentine (*m/z* 349), ajmalicine (*m/z* 353), methoxy tabersonine (*m/z* 367), lochnerinine (*m/z* 383), echitovenine (*m/z* 397), deacetoxy vindoline (*m/z* 399), vindolidine (*m/z* 427), strictosidine (*m/z* 531), anhydrovinblastine (*m/z* 793), and vinblastine (*m/z* 811). As many of the names of natural products are uncommon in regular analytical chemistry literature, we have summarized in Table S1 of the Supporting Information the essential details of the compounds discussed in this work. Besides alkaloids, the other peaks that eluted (e.g., *m/z* 88, 112, 144, 188, 203, 219, and 233) could be similarly assigned by their MS/MS data by referring to the other metabolic pathways in KEGG database. It may be noted that the mass accuracies mentioned in Table S1 refer to the database and not from the present study. As plethora of information is available for *Catharanthus* in different databases,[18−22] we did not attempt other experiments for separation, characterization, structural identification for molecular variations/relationships, etc. The periwinkle plant(s) collected from different locations were imaged, but the predominant and the coexisting peaks expressed on these surfaces did not change thereby confirming the reproducibility of our results.

To identify the changes in metabolites at various growth stages, the leaves of *C.roseus* at seedling and senescent stages were imaged. Vindoline (*m/z* 457), a predominant metabolite in leaves (Figure 2B), is reported to be confined to aerial parts of plants and is not produced in cultures.[28] Here imaging of healthy, young, and mature leaves of *C. roseus* showed the relative abundance of vindoline (*m/z* 457) but the predominance of *m/z* 339 is seen in newly emerged leaf of young seedlings[19] (Figure 4A). In the senescing leaf (Figure 4B), there was predominance of *m/z* 337 over *m/z* 457.

Imaging changes in metabolites during growth stages has implication in agricultural and food crops. The toxic metabolites that need to be monitored may be produced in plants during early stages of growth (e.g., a natural toxin-glycoalkaloid(s) in Solanaceous crops such as potato, tomato)[29] or during senescence (as in tobacco, the back conversion of nicotine to nornicotine leading to the formation of a carcinogenic precursor N′-nitrosonornicotine).[30] Though the toxicities of glycoalkaloids is well known, their bioactivities,[29] particularly the anticancer activity, are desirable.[31−34] The variation in content of glycoalkaloid[35] is found in plant parts, particularly in leaves where metabolic activity is more; hence testing for glycoalkaloid content is mandatory at different stages. Figure 4C shows that imaging techniques may be a rapid method in identifying the spatial distribution of α-solanine and α-chaconine, the two crucial glycoalkaloids in very young seedlings of potato.[31] When a mature leaf of tomato was imaged, the distribution of typical glycoalkaloid peaks for α-tomatine (*m/z* 1034.7 and 528.9)[33] was evident as shown in Figure 4D.

DESI MS imaging is used in the detection of pathogens;[36] here the possibility to view metabolites particularly at the site of pest attack (*m/z* 337 in Figure 5A: chewing pest, grasshopper attack on petal) and pathogen attack (*m/z* 793 in Figure S3A, Supporting Information: leaf spot disease on leaf) are shown. Figure 5B shows metabolite changes during wilt disease on leaf.

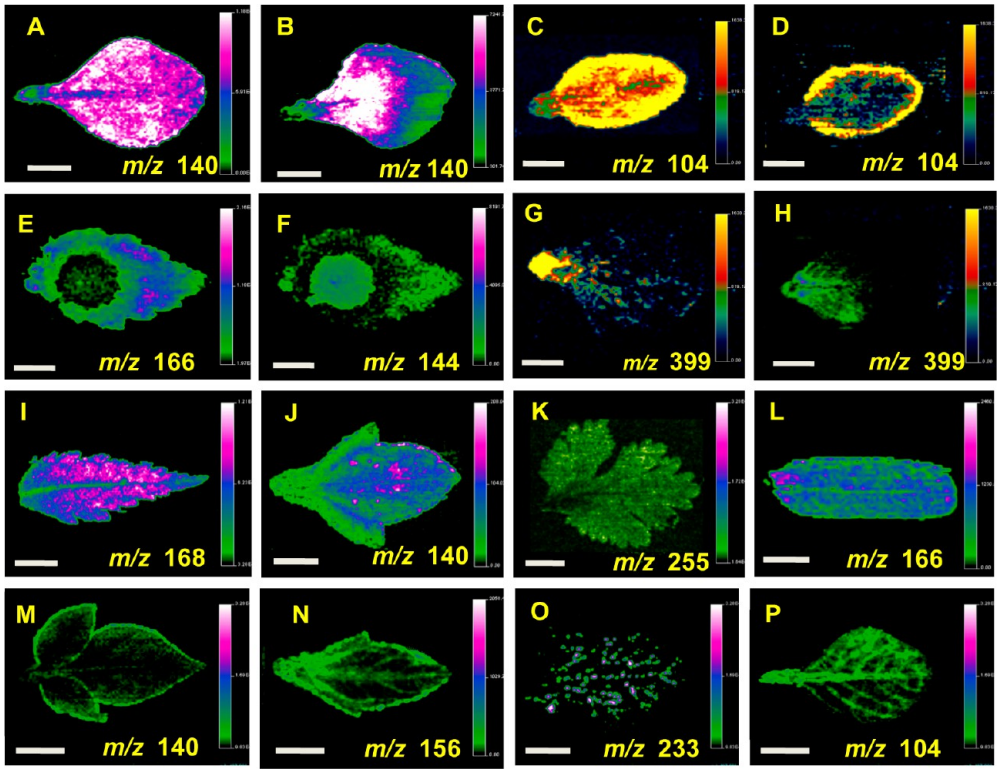

Figure 6. DESI MS images showing (A, B) difference in distribution of m/z 140 on the lower surface of leafy vegetable amaranthus for identification from weed admixtures, (C, D) difference in distribution of m/z 104 on rosette and cauline leaves of tissue cultured *Arabidopsis thaliana*, (E, F) location of secretory gland in leaf of patchouli, (G, H) distribution of eye color imparting metabolite (m/z 399) in petal and leaf of *C. roseus*, (I, J, K, L) typical leaf shape in neem, wedelia, coriander, and tamarind, respectively, and (M, N, O, P) spatial distribution showing metabolites present on the leaf margin and veins on potato, wedelia, coriander, and amaranthus, respectively . The scale is uniform in all the images (5 mm).

Figure S3B in the Supporting Information shows the changes in spatial distribution of m/z 349 during aphid attack on the lower surface of the leaf. It is interesting to note that the changes in the relative abundance of peaks m/z 349, m/z 397, and m/z 793 were observed in all of those cases (Figure 5A,B, and Figure S3A,B) besides changes in intensity of m/z 337 and m/z 457. Although some peaks in ESI spectra were having very low intensity, their surface images were pronounced in DESI MS, implying their stable expression in nature and also their relationship with the prominent compounds (Figure 5C). In order to avoid loss of data, baseline correction or statistical methods were not applied.

Though flower of *C. roseus* is actinomorphic (Figure 1A,B), some atrophied flowers (Figure S1C, with changes in shapes, size, and color of petals) were observed during environmentally stressed conditions in naturally growing plants. As the upper surfaces showed specific changes, the TLC-imprint (no. 6 of Figure S1C) of an atrophied flower is imaged and results are given in Figure 5D. The changes in spatial distribution of alkaloids (m/z 349, m/z 397, and m/z 793) and other metabolites (m/z 203, m/z 219, and m/z 427) can be observed in images 6−10 of Figure 5D. The spatial distribution of commonly known Catharanthus alkaloids in petal or leaf (Figure 2A,B) is indeed new information from this study. Their coexistence with other phenolic compounds and the expression in pest/pathogen attack or abiotic stress will add to the existing knowledge[37−39] that these could be looked at as biomarker metabolites in biotic and abiotic stresses. Hence imaging plant surfaces, immediately after finding changes on their physical features, may serve as a rapid test to identify molecular signatures in stress and to take suitable prophylactic measures for saving crop plants.

The spatial distribution of particular metabolite(s) between different colored varieties of *C. roseus* (Figure 1D,E) shows that imaging can help in comparing different varieties or species. Identification of leafy vegetable amaranthus types remains a challenge due to admixtures with weeds.[40] As in Figure 6A,B, imaging the upper and lower surfaces of leaves show a difference in spatial distribution of metabolites which may be significant in identifying vegetable amaranthus leaf from the weed admixtures.

Parts C and D of Figure 6 show the spatial distribution of metabolite (m/z 104) in two different types of leaves in the same plant (cauline and rosette leaves in tissue cultured *Arabidopsis thaliana*). Here tissue cultured *Arabidopsis* plants are chosen because enhancing the production of bioactive molecules through tissue culture or in vitro manipulations is done in different plant varieties.

Very subtle features on the surface of leaves and petals that are not visible in photographs of TLC-imprints are reflected in DESI MS images. For example, Figure 6E,F shows the presence of vacuole or subsurface secretory gland in the leaf of patchouli,[41] which is invisible in its TLC-imprint (Figure S1B, no.6). The spatial distribution images of the undamaged vacuole/secretory gland in patchouli leaf shows that the pressure is not emptying the contents on TLC-imprints. Likewise, the metabolite (m/z 399) imparting color to visible patterns on the flower eye of *C. roseus* was imaged (as in image 7 of Figure 5D for flower and in Figure 6G for petal); though invisible in the TLC-imprint of leaf, Figure 6H shows that the

dx.doi.org/10.1021/jf4011998 | J. Agric. Food Chem. 2013, 61, 7477−7487

metabolite (m/z 399) is confined to the base of the leaf. As in Figure 6I−L, the typical/conspicuous leaf shapes (serrated margin of neem, trilobed shape of wedelia, parsley leaf like shape of coriander) of plants can be imaged. Parts M−P of Figure 6 show the presence of metabolite peak at leaf veins and margin, which unravels the possibilities to image diseases expressed on leaf veins or margins.[42]

Though TLC-imprints produce flat surfaces, there are possibilities of defects in images arising from imprints due to manual errors as with improper pressing (Figure S4A). Also, the surface changes in TLC-imprints during storage (Figure S4B) produced time-dependent variations in images; the changes were evident in petal imprints within a few days but leaf imprints lasted for months. Also, there may be defects in imaging (Figure S4C) due to the instrumental setting errors.[43] In addition, the interfering peaks sometimes masked the presence of predominant metabolite image(s) (Figure S4D). As plants are complex, no single method can be fully effective to understand plant system biology or plant molecular signatures at a given time. Hence new methods[44] may be employed to better interpret the results obtained from the DESI MS imaging technique. Since all biological samples are highly variable due to changes in edaphic and climatic conditions, the results given here may vary depending on a number of factors including tropical and temperate growth variations. Even the plant metabolite profile database created for the model plant *Arabidopsis* is not complete.[45] Moreover, the TLC-imprinting method needs to be modified suitably for other plant parts like stem, root, seed, etc., and an amenable strategy is needed for imprinting leathery textured leaves and latex containing plants. With suitable manipulations to overcome these limitations, this method would be useful for preserving the molecular information of plant species. As imprints can be transported and stored at ease, this methodology will become useful in herbarium documentation.

■ ASSOCIATED CONTENT

Supporting Information

Additional figures and table as described in the text. This material is available free of charge via the Internet at http://pubs.acs.org.

■ AUTHOR INFORMATION

Corresponding Author

*Tel.: +91-044-2257 4208. Fax: +91-044-2257 0545/0509. E-mail: pradeep@iitm.ac.in.

Funding

Financial support is from the Department of Science and Technology (DST) and the Department of Biotechnology, Government of India.

Notes

The authors declare no competing financial interest.

■ ACKNOWLEDGMENTS

The authors thank Prof. M. Vasundhara of GKVK campus, University of Agricultural Sciences, Bangalore, for providing the patchouli plants, and Dr. R. Baskar of IIT Madras for providing the tissue cultured *Arabidopsis* plants. T.P. thanks the Department of Science and Technology, Government of India, for equipment support through the Nano Mission.

■ REFERENCES

(1) Lee, Y. J.; Perdian, D. C.; Song, Z.; Yeung, E. S.; Nikolau, B. J. Use of mass spectrometry for imaging metabolites in plants. *Plant J.* **2012**, *70*, 81−95.

(2) Takats, Z.; Wiseman, J. M.; Gologan, B.; Cooks, R. G. Mass spectrometry sampling under ambient conditions with desorption electrospray ionization. *Science* **2004**, *306*, 471−473.

(3) Kauppila, T. J.; Talaty, N.; Salo, P. K.; Kotiaho, T.; Kostiainen, R.; Cooks, R. G. New surfaces for desorption electrospray ionization mass spectrometry: porous silicon and ultra-thin layer chromatography plates. *Rapid Commun. Mass Spectrom.* **2006**, *20*, 2143−2150.

(4) Muller, T.; Oradu, S.; Ifa, D. R.; Cooks, R. G.; Krautler, B. Direct plant tissue analysis and imprint imaging by desorption electrospray ionization mass spectrometry. *Anal. Chem.* **2011**, *83*, 5754−5761.

(5) Badu-Tawiah, A.; Bland, C.; Campbell, D. I.; Cooks, R. G. Non-aqueous spray solvents and solubility effects in desorption electrospray ionization. *J. Am. Soc. Mass Spectrom.* **2010**, *21*, 572−579.

(6) Liu, J.; Wang, H.; Cooks, R. G.; Ouyang, Z. Leaf spray: Direct chemical analysis of plant material and living plants by mass spectrometry. *Anal. Chem.* **2011**, *83*, 7608−7613.

(7) Peng, Y.e; Zhang, S.; Wen, F.; Ma, X.; Yang, C.; Zhang, X. In vivo nanoelectrospray for the localization of bioactive molecules in plants by mass spectrometry. *Anal. Chem.* **2012**, *84*, 3058−3062.

(8) Grieving, M. P.; Patti, G. J.; Siuzdak, G. Nanostructure-Initiator mass spectrometry metabolite analysis and imaging. *Anal. Chem.* **2011**, *83*, 2−7.

(9) Joyce, N. I.; Eady, C. C.; Silcock, P.; Perry, N. B.; van Klink, J. W. Fast phenotyping of LFS-silenced (tearless) onions by desorption electrospray ionization mass spectrometry (DESI-MS). *J. Agric. Food Chem.* **2013**, *61*, 1449−1456.

(10) O'Connor, S. E.; Maresh, J. Chemistry and biology of monoterpene indole alkaloid biosynthesis. *J. Nat. Prod. Rep.* **2006**, *23*, 532−547.

(11) Ifa, D. R.; Srimany, A.; Eberlin, L. S.; Naik, H. R.; Bhat, V.; Cooks, R. G.; Pradeep, T. Tissue imprint imaging by desorption electrospray ionization mass spectrometry. *Anal. Methods* **2011**, *3*, 1910−1912.

(12) Li, B.; Bjarnholt, N.; Hansen, S. H.; Janfelt, C. Characterization of barley leaf tissue using direct and indirect desorption electrospray ionization imaging mass spectrometry. *J. Mass Spectrom.* **2011**, *46*, 1241−1246.

(13) Thunig, J.; Hansen, S. H.; Janfelt, C. Analysis of Secondary plant metabolites by indirect desorption electrospray ionization imaging mass spectrometry. *Anal. Chem.* **2011**, *83*, 3256−3259.

(14) http://spectra.psc.riken.jp/menta.cgi/search/fragment.

(15) http://metlin.scripps.edu/spec_search.php.

(16) Horai, H.; Arita, M.; Kanaya, S.; Nihei, Y.; Ikeda, T.; Suwa, K.; Ojima, Y.; Tanaka, K.; Tanaka, S.; Aoshima, K.; Oda, Y.; Kakazu, Y.; Kusano, M.; Tohge, T.; Matsuda, F.; Sawada, Y.; Hirai, M. Y.; Nakanishi, H.; Ikeda, K.; Akimoto, N.; Maoka, T.; Takahashi, H.; Ara, T.; Sakurai, N.; Suzuki, H.; Shibata, D.; Neumann, S.; Iida, T.; Funatsu, K.; Matsuura, F.; Soga, T.; Taguchi, R.; Saito, K.; Nishioka, T. MassBank: a public repository for sharing mass spectral data for life sciences. *J. Mass Spectrom.* **2010**, *45*, 703−714.

(17) Ferreres, F.; Pereira, D. M.; Valentao, P.; Oliveira, J. M.; Faria, J.; Gaspar, L.; Sottomayor, M.; Andrade, P. B. Simple and reproducible HPLC-DAD-ESI-MS/MS analysis of alkaloids in Catharanthus roseus roots. *J. Pharm. Biomed. Anal.* **2010**, *51*, 65−69.

(18) Van Moerkercke, A.; Fabris, M.; Pollier, J.; Baart, G. J.; Rombauts, S.; Hasnain, G.; Rischer, H.; Memelink, J.; Oksman-Caldentey, K. M.; Goossens, A. CathaCyc, a metabolic pathway database built from Catharanthus roseus RNA-Seq data. *Plant Cell Physiol.* **2013**, *54*, 673−685.

(19) http://metnetdb.org/mpmr_public/experiments/?expid=139 (accessed on June 8, 2013).

(20) http://www.biologie.uni-freiburg.de/data/bio2/schroeder/Index_English_Catharanthus.html (accessed on June 8, 2013).

(21) http://www.genome.jp/kegg/pathway/map/map00901.html (accessed on June 8, 2013).

(22) http://www.ncbi.nlm.nih.gov/pccompound (accessed on June 8, 2013).
(23) Sharma, V.; Walia, S.; Kumar, J.; Nair, M. G.; Parmar, B. S. An efficient method for the purification and characterization of nematicidal azadirachtins A, B, and H, using MPLC and ESIMS. *J. Agric. Food Chem.* **2003**, *51*, 3966−3972.
(24) That, Q. T.; Jossang, J.; Jossang, A.; Kim, P. P. N.; Jaureguiberry, G. Wedelolides A and B: Novel sesquiterpene δ-lactones, (9R)-eudesman-9,12-olides, from *Wedelia trilobata*. *J. Org. Chem.* **2007**, *72*, 7102−7105.
(25) Sudjaroen, Y.; Haubner, R.; WÃ1/4rtele, G.; Hull, W. E.; Erben, G.; Spiegelhalder, B.; Changbumrung, S.; Bartsch, H.; Owen, R. W. Isolation and structure elucidation of phenolic antioxidants from tamarind (*Tamarindus indica* L.) seeds and pericarp. *Food Chem. Toxicol.* **2005**, *43*, 1673−1682.
(26) Tozuka, Z.; Kaneko, H.; Shiraga, T.; Mitani, Y.; Beppu, M.; Terashita, S.; Kawamura, A.; Kagayama, A. Strategy for structural elucidation of drugs and drug metabolites using (MS)n fragmentation in an electrospray ion trap. *J. Mass Spectrom.* **2003**, *38*, 793−808.
(27) Keglevich, P.; Hazai, L.; Kalaus, G.; Szantay, C. Modifications on the basic skeletons of vinblastine and vincristine. *Molecules* **2012**, *17*, 5893−5914.
(28) Guirimand, G.; Guihur, A.; Poutrain, P.; Hericourt, F.; Mahroug, S.; St-Pierre, B.; Burlat, V.; Courdavault, V. Spatial organization of the vindoline biosynthetic pathway in *Catharanthus roseus*. *J. Plant Physiol.* **2011**, *168*, 549−557.
(29) Milner, S. E.; Brunton, N. P.; Jones, P. W.; O'Brien, N. M.; Collins, S. G.; Maguire, A. R. Bioactivities of glycoalkaloids and their aglycones from *Solanum* species. *J. Agric. Food Chem.* **2011**, *59*, 3454−3484.
(30) Siminszky, B.; Gavilano, L.; Bowen, S. W.; Dewey, R. E. Conversion of nicotine to nornicotine in *Nicotiana tabacum* is mediated by CYP82E4, a cytochrome P450 monooxygenase. *Proc. Natl. Acad. Sci. U.S.A.* **2005**, *102*, 14919−14924.
(31) Matsuda, F.; Morino, K.; Miyazawa, H.; Miyashita, M.; Miyagawa, H. Determination of potato glycoalkaloids using high-pressure liquid chromatography−electrospray ionisation/mass spectrometry. *Phytochem. Anal.* **2004**, *15*, 121−124.
(32) Reddivari, L.; Vanamala, J.; Safe, S. H.; Miller, J. C., Jr. The bioactive compounds alpha-chaconine and gallic acid in potato extracts decrease survival and induce apoptosis in LNCaP and PC3 prostate cancer cells. *Nutr. Cancer.* **2010**, *62*, 601−610.
(33) Cataldi, T. R.; Lelario, F.; Bufo, S. A. Analysis of tomato glycoalkaloids by liquid chromatography coupled with electrospray ionization tandem mass spectrometry. *Rapid Commun. Mass Spectrom.* **2005**, *19*, 3103−3110.
(34) Choi, S. H.; Lee, S. H.; Kim, H. J.; Lee, I. S.; Kozukue, N.; Levin, C. E.; Friedman, M. Changes in free amino acid, phenolic, chlorophyll, carotenoid, and glycoalkaloid contents in tomatoes during 11 stages of growth and inhibition of cervical and lung human cancer cells by green tomato extracts. *J. Agric. Food Chem.* **2010**, *58*, 7547−7556.
(35) Itkin, M.; Rogachev, I.; Alkan, N.; Rosenberg, T.; Malitsky, S.; Masini, L.; Meir, S.; Iijima, Y.; Aoki, K.; de Vos, R.; Prusky, D.; Burdman, S.; Beekwilder, J.; Aharoni, A. GLYCOALKALOID METABOLISM1 is required for steroidal alkaloid glycosylation and prevention of phytotoxicity in tomato. *Plant Cell* **2011**, *23*, 4507−4525.
(36) Lane, A. L.; Nyadong, L.; Galhena, A. S.; Shearer, T. L.; Stout, E. P.; Parry, R. M.; Kwasnik, M.; Wang, M. D.; Hay, M. E.; Fernandez, F. M.; Kubanek, J. Desorption electrospray ionization mass spectrometry reveals surface-mediated antifungal chemical defense of a tropical seaweed. *Proc. Natl. Acad. Sci. U. S. A.* **2009**, *106*, 7314−7319.
(37) Vazquez-Flota, F.; Carrillo-Pech, M.; Minero-Garcia, Y.; De Lourdes Miranda-Ham, M. Alkaloid metabolism in wounded *Catharanthus roseus* seedlings. *Plant Physiol. Biochem.* **2004**, *42*, 623−628.
(38) Roepke, J.; Salim, V.; Wu, M.; Thamm, A. M.; Murata, J.; Ploss, K.; Boland, W.; De Luca, V. Vinca drug components accumulate exclusively in leaf exudates of Madagascar periwinkle. *Proc. Natl. Acad. Sci. U.S.A.* **2010**, *107*, 15287−15292.
(39) Ferreres, F.; Figueiredo, R.; Bettencourt, S.; Carqueijeiro, I.; Oliveira, J.; Gil-Izquierdo, A.; Pereira, D. M.; Valentao, P.; Andrade, P. B.; Duarte, P.; Barcelo, A. R.; Sottomayor, M. Identification of phenolic compounds in isolated vacuoles of the medicinal plant *Catharanthus roseus* and their interaction with vacuolar class III peroxidase: an H(2)O(2) affair? *J. Exp. Bot.* **2011**, *62*, 2841−2854.
(40) Khan, M.; Musharaf, S.; Ibrar, M.; Hussain, F. Pharmacognostic evaluation of the *Amaranthus viridis* L. *Res. Pharm. Biotechnol.* **2011**, *3*, 11−16.
(41) Maeda, E.; Miyake, H. Leaf anatomy of patchouli with reference to the disposition of mesophyll glands. *Jpn. J. Crop Sci.* **1997**, *66* (2), 307−317.
(42) Cazorla, F. M.; Vázquez, M. A.; Rosales, J.; Arrebola, E.; Navarro, J.; Pérez-García, A.; De Vicente, A. First report of bacterial leaf spot (*Pseudomonas syringae* pv. *coriandricola*) of coriander in Spain. *J. Phytopathol.* **2005**, *153*, 181−184.
(43) Kertesz, V.; Van Berkel, G. J. Scanning and surface alignment considerations in chemical imaging with desorption electrospray mass spectrometry. *Anal. Chem.* **2008**, *80*, 1027−1032.
(44) Campbell, D.; Ferreira, C.; Eberlin, L.; Cooks, R. G. Improved spatial resolution in the imaging of biological tissue using desorption electrospray ionization. *Anal. Bioanal. Chem.* **2012**, *404*, 389−398.
(45) Bais, P.; Moon-Quanbeck, S. M.; Nikolau, B. J.; Dickerson, J. A. Plantmetabolomics.org: mass spectrometry-based *Arabidopsis* metabolomics–database and tools update. *Nucleic Acids Res.* **2012**, *40* (Database issue), D1216−20.